Density Functional Study of Chromium Oxide Clusters: Structures, Bonding, Vibrations, and Stability

Sundar Veliah, Kai-hua Xiang, Ravindra Pandey,* J. M. Recio, and John M. Newsam†

Department of Physics, Michigan Technological University, Houghton, Michigan 49931

Received: August 5, 1997; In Final Form: November 5, 1997

We report the results of density functional theory calculations on chromium oxide clusters responding to the formula Cr_mO_n ($m = 1-2$, $n = 1-3$). Double numeric basis sets supplemented by polarization functions have been used in both local and nonlocal spin density approximations. Geometry optimizations of different spin states have been performed at the unrestricted spin level for the selected initial configurations. We have found that the covalent polarized Cr−O bonds dominate the chemical description of the CrO_n series, while for the Cr_2O_n series the presence of the Cr−Cr bond reduces the metal to oxygen charge transfer, yielding much softer clusters, as reflected by the smaller HOMO−LUMO gaps. The stability of all the isomers has been checked by computing their harmonic vibrational frequencies and the energetics of different fragmentation paths. The calculations reveal that the linear isomers are not true minima and that the oxygen-rich clusters are preferred over the metal-rich clusters. Overall, our results show good agreement with the available experimental data in terms of geometrical parameters, vibrational frequencies, atomization energies, and fragmentations for the CrO_n clusters. For the Cr_2O series, our computed values are discussed in connection with recent infrared spectroscopy measurements and with available data in analogous metal oxide clusters.

1. Introduction

Transition metal oxides have been extensively studied in their bulk states, but despite substantial interest from a catalytic perspective, very little attention has been paid to their cluster counterparts. Relative to oxides of main group elements, involvement of d orbitals in bonding makes the chemistry of transition metal oxides diverse and leads to a range of technological applications. For example, the oxides of chromium are used to catalyze the polymerization of olefins and as a coating material for magnetic recording applications.[1] On the other hand, these systems with a large number of open-shell electrons have shown to be highly difficult to handle from a theoretical point of view.[2]

The experimental work carried out so far on transition metal oxide clusters can be classified in two areas according to their objectives. The first area focuses on the determination of the composition, building blocks, abundance patterns, and fragmentation routes of clusters that usually contain a large number of atoms. It is common to find multiphoton ionization and mass spectrometry as the experimental techniques applied in these works. The other one is directed to the determination of structural parameters, vibrational frequencies, electron affinities, and the description of the bonding and the electronic structure of small clusters by means of infrared, Raman, and photoelectron spectroscopies. Preparation methods to generate clusters are found to be independent of the types of experimental studies. In the more recent investigations, chromium oxide clusters are generated by oxidation of laser-ablated Cr atoms,[3−5] whereas in earlier investigations the preparation involved the vaporization of crystalline Cr_2O_3[6] and the photolysis of $Cr(CO)_6$ in O_2-doped argon matrixes.[7]

Concerning the first area, it has been found that (a) oxide clusters of vanadium, chromium, and iron show abundance of oxygen-rich cluster peaks in the mass spectra and (b) for these clusters the oxygen-to-metal ratio assumes a constant value with increasing cluster size.[3] Metal-rich clusters, on the other hand, are found to dominate the mass spectra of nickel oxide clusters.[3] In manganese oxide, mass spectroscopic studies[8] indicate the stable structures to be $(MnO)_n$ clusters with $n = 3$, 6, 9, and 12. These compositions follow closely the stoichiometry of the high-temperature species in the corresponding metal−oxygen diagrams.

The focus on the characterization of the particular Cr_mO_n clusters containing less than 10 atoms have experienced a renewed interest very recently. Thus, the CrO_2 molecule has been the subject of ultraviolet photoelectron[4] and infrared[5] spectroscopy experiments that lead to a greater O−Cr−O angle than the one reported before[7] and to a more accurate determination of molecular vibrational frequencies. The work of Chertihin et al.[5] has also posed a number of interesting questions concerning the geometrical configurations and the frequency assignments of the Cr_mO_n ($m = 1-2$, $n = 1-4$) clusters. For example, the estimated value of bond angle of 138° for Cr_2O seems to be too high, given the role that the Cr−Cr bond should play in the chemistry of chromium-rich clusters.

As regards the theoretical approaches utilized to understand the properties of clusters containing transition metals, there has been discussions whether Hartree−Fock (HF) and post-HF methods were more appropriate or not than alternatives based on the density functional theory (DFT). Some controversy has been focused on the Cr_2 dimer in the early 1980's.[9] More recently, Torrent et al.[2] have undertaken an exhaustive investigation using both types of methodologies to explore CrO_2X_2 (X = F, Cl, Br, I) compounds and have concluded that DFT

† Molecular Simulations Inc., San Diego, CA 92121.

S1089-5647(97)02546-7 CCC: $15.00
Published on Web 01/27/1998

procedures are more suitable when balance between accuracy of results and computational costs is required.

DFT calculations at the local spin density level on similar sizes as the ones considered here, but for Cu_2O_n ($n = 1-4$) clusters, have shown to be an efficient tool to interpret and complement photoelectron spectroscopy studies of size-selected clusters.[10] For CrO_2, calculations based on DFT have also been performed to characterize its geometry and as a guide for vibrational frequency assignments.[5] Besides CrO_2, we are not aware of any previous theoretical studies performed on chromium oxide clusters, except the extensive work on the diatomic molecule.[11-13]

In this paper, we consider small clusters of chromium oxide, both oxygen-rich and metal-rich, namely, CrO, CrO_2, CrO_3, Cr_2O, Cr_2O_2, and Cr_2O_3, in the framework of the density functional theory using both local and nonlocal spin exchange and correlation functionals. We pursue a fourfold objective: (i) The determination of the ground states and their structural parameters for the above clusters. This task involves total energy calculations of size-selected configurations in different spin states and global geometrical optimizations. (ii) The understanding of the trends in the chemical bonding of the lowest energy isomers in the CrO_n and Cr_2O_n series and the differences between them. This study is performed through the analysis of molecular orbital energies and coefficients, electronic density maps, and density of state plots. (iii) The interpretation of the computed harmonic vibrational frequencies and normal modes in relation with recent available experimental data for these Cr_mO_n clusters and with data of analogous aggregates. (iv) The exploration of the fragmentation paths that inform on the relative stability of the clusters under study.

The paper is organized as follows: Section 2 describes the computational aspects of our calculations using the CrO molecule as a test case to check the parameters of the method. Section 3 contains the results and the discussion and is divided in three subsections that deal with molecular structures, chemical bonding, and stability of the clusters. Finally, we present the conclusions of our study in the last section.

2. Methodology

Many electron calculations on the Cr_mO_n ($m = 1-2$, $n = 1-3$) clusters are performed using the program DMol[14] at the unrestricted spin level in the local and nonlocal spin density approximations. The sensitivity of the computational procedure to the parameters employed was explored by studying, in detail, the effects of using different local and nonlocal functionals and of freezing different core orbitals on the structure and energetics of these clusters. Comparison with experimental and other theoretical results on CrO provides a test of the model elements of the present work.

In all the calculations, we have used double numeric basis sets (DNP) supplemented by diffuse and polarization functions (4p for Cr and 3d for O). The size of the DNP basis set is comparable with a polarized double-ζ basis set, although it should be noticed that exact atomic functions are used here and, therefore, a higher quality can be associated with the DNP basis sets. The accuracy of the DNP basis set has been analyzed in detail by Delley,[15,16] and such basis sets have been used successfully to study the nature of bonding in the Cr_2 molecule,[15] the structure and energetics of Cu clusters,[17] and MgO clusters.[18] The appropriate choice of local or nonlocal functionals is also important, and we have investigated the effects of different local and nonlocal potentials on some basic properties of CrO (Table 1). In particular, we have considered the Hedin-Lundqvist/Janak-Moruzzi-Williams (JMW)[19] and the Vosko-Wilk-Nusair (VWN)[20] local functionals. As nonlocal potentials, we have considered a combination of gradient corrected exchange functional of Becke[21] with the Perdew-Wang gradient corrected correlation functional (BPW)[22] and with Vosko, Wilk, and Nusair's local correlation functional (BVWN).

TABLE 1: Summary of Results for CrO($^5\Pi$)

	R_{eq} (Å)	D_e (eV)	ω_e (cm^{-1})	μ (D)	Cr Mulliken charge
this work (DFT)					
local (JMW)	1.60	5.93	996	3.66	0.63
local (VWN)	1.60	6.15	976	3.76	0.63
nonlocal (BVWN)	1.64	5.12	884	4.01	0.64
nonlocal (BPW)	1.63	5.18	961	3.82	0.63
other calculations					
MC-SCF[a]	1.86	2.52	630		0.63
MR-CISD[a]	1.66	3.09	820		0.53
MC-SCF[b]	1.657	3.86	821	2.7	
MR-CISD[b]	1.647	4.00	850	3.2	
experiment[c]	1.615	4.41 ± 0.30	898	3.88 ± 0.13	

[a] Reference 11. [b] Reference 23. [c] Quoted by ref 12.

The data collected in Table 1 reveal that (i) the form of potentials chosen for the exchange and correlation functionals only produce a small scattering in the values of the computed magnitudes and (ii) the agreement with the experimental data and the comparison with accurate post-HF calculations is very reasonable. These two facts allow us to proceed with the computations in larger clusters using any of these tested potentials. Nevertheless, to make the calculations feasible and to present clearly the ongoing results, we have selected two of the above four alternatives. For the local spin density approximation (LSDA), the choice is the VWN functional, whereas the Becke/VWN functionals will be used for nonlocal spin density approximation (NLSDA). From a theoretical perspective, the use of nonlocal corrections is more desirable and has proven to give a better agreement with the experimental data (see Table 1). Therefore, hereafter a greater focus is given for the results obtained in NLSDA computations.

The effects of freezing the core orbitals (i.e., argon core is frozen for chromium and helium core is frozen for oxygen) on the bond length, dissociation energy, and vibrational frequency of CrO were found to be negligible, and this approximation was therefore adopted for subsequent calculations. The density and energy tolerances were set to 10^{-5} e/bohr^3 and 10^{-8} hartree, respectively. The vibrational frequencies were computed by a double point finite differencing formula with a step size of 0.1 bohr.

3. Results and Discussion

3.1. Structural Properties. The structural parameters of the CrO_n and Cr_2O_n ($n = 1-3$) clusters after LSDA and NLSDA optimizations are given in Tables 2 and 3, respectively. The low-lying spin states (i.e., singlet, triplet, quintet, and septet) of a given cluster were considered in the calculations. The optimized configurations of the lowest energy isomers in their respective ground states are shown in Figure 1. In the rest of this subsection, we only analyze the NLSDA results. Comparison with the LSDA results may be easily carried out following general considerations: the lowering of the total energy of the clusters in NLSDA and the small increase in distances and angles in NLSDA. Note that the spin states and isomers with the lowest energies for each cluster are found to be the same in both LSDA and NLSDA calculations.

TABLE 2: Calculated Structural Parameters of CrO_n Clusters ($n = 1-3$)

cluster	multiplicity ($2S+1$)	R_{Cr-O} (Å)	R_{O-O} (Å)	O−Cr−O angle (deg)	total energy (hartrees)
		Local (VWN)			
CrO, $C_{\infty v}$	1	1.55			−1116.913 15
	3	1.56			−1116.941 77
	5	1.60			−1116.971 74
CrO_2, C_{2v}	1	1.58	2.65	113.7	−1191.738 52
	3	1.59	2.78	121.6	−1191.768 47
	5	1.64	3.12	143.5	−1191.682 72
CrO_3, C_{3v}	1	1.59	2.64	112.7	−1266.538 09
	3	1.62	2.74	115.4	−1266.484 68
	5	1.77	2.26	79.4	−1266.280 22
		Nonlocal (BVWN)			
CrO, $C_{\infty v}$	1	1.61			−1120.917 86
	3	1.61			−1120.945 19
	5	1.64			−1120.976 14
CrO_2, C_{2v}	1	1.63	2.85	122.5	−1196.519 86
	3	1.64	2.98	131.1	−1196.553 71
	5	1.69	3.25	148.2	−1196.479 95
CrO_3, C_{3v}	1	1.62	2.74	115.0	−1272.098 06
	3	1.66	2.88	119.5	−1272.054 22
	5	1.85	3.09	113.5	−1271.866 61

3.1.1. CrO, CrO_2, and CrO_3. As commented before, NLSDA yields values for the bond length, frequency, dissociation energy, and dipole moment of CrO that are in good agreement with earlier experimental and theoretical studies, as illustrated in Table 1. Results calculated in LSDA give a higher value for the dissociation energy but more accurate value for the Cr−O bond length. The error in the LSDA dissociation energy is as expected; LSDA is known to overestimate binding energies. On the other hand, NLSDA corrects for this overestimation and yields a bond length and dissociation energy that are within 1% and 10%, respectively, of the corresponding experimental values (see ref 12). In comparison, the ab initio configuration interaction (CI) calculation gives an error of about 8% for the dissociation energy attributed to the large differential correlation effects.[23] The NLSDA vibrational frequency is very close to the experimental result. The calculated NLSDA value of the dipole moment is 4.00 D in comparison to the multireference-CI singles and doubles (MR-CISD) value of 3.2 D.[23] More recent theoretical and experimental studies on the CrO molecule have found the dipole moment to be 3.88 ± 0.13 D.[12,24] Both LSDA and NLSDA yield the valence configuration of the ground state to be $5\sigma^2 6\sigma^1 2\pi^4 3\pi^1 1\delta^2$ ($^5\Pi$), in accordance with previous experiments and theoretical calculations.

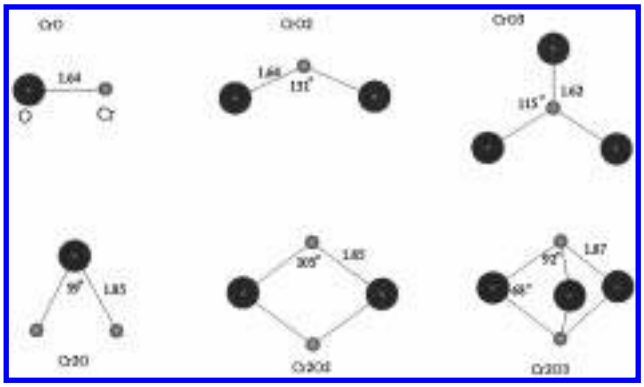

Figure 1. Optimized configurations of the ground states of chromia clusters obtained in the nonlocal spin density approximation.

For CrO_2, the bent configuration having C_{2v} symmetry is found to be lower in energy than the linear isomer, in agreement with infrared and photoelectron spectroscopy studies.[4,5,7] The recent experimental values for the O−Cr−O bond angle have ranged from 112 ± 2° (ref 7) to 128 ± 5° (ref 5). Our computed NLSDA value is 131.1°, in very good agreement with the one proposed after the latest infrared experiments. As far as we know, the only theoretical result for the bond angle of this molecule is 125° (ref 5). In their preliminary theoretical work, Chertihin et al. explored several configurations for this triatomic molecule and, as in our work, found that the C_{2v} isomer in the triplet spin state is the one with the lowest energy.[5] Slight differences appear when we compare the corresponding R_{Cr-O} distance. Whereas in their calculations a reduction from the monomer of 0.03 Å is predicted, in our NLSDA calculations the distance remains the same in the monomer and in the triatomic. Besides, our NLSDA value for the O−O separation becomes 0.7 Å greater than in the O_2 molecule, which predicts the negligible role of the O−O bonding in these clusters.

Addition of a new oxygen atom to the triatomic molecule produces a lowest energy isomer with a nonplanar structure, where the chromium atom is only 0.349 Å above the plane

TABLE 3: Calculated Structural Parameters of Cr_2O_n Clusters ($n = 1-3$)

	multiplicity ($2S+1$)	R_{Cr-O} (Å)	R_{O-O} (Å)	R_{Cr-Cr} (Å)	Cr−O−Cr angle (deg)	O−Cr−O angle (deg)	total energy (hartrees)
				Local (VWN)			
Cr_2O, C_{2v}	1	1.84		1.69	54.7		−2159.261 72
	3	1.79		1.78	59.3		−2159.267 53
	5	1.80		1.89	63.3		−2159.247 82
Cr_2O_2, D_{2h}	1	1.76	2.94	1.94	66.7	113.3	−2234.076 02
	3	1.77	2.95	1.95	66.9	113.1	−2234.075 34
	5	1.76	2.79	2.16	75.3	104.7	−2234.070 28
	7	1.79	2.81	2.21	76.3	103.7	−2234.089 56
Cr_2O_3, D_{3h}	1	1.77	2.41	2.19	76.4	85.8	−2308.841 31
	3	1.79	2.48	2.13	73.3	88.0	−2308.829 59
	5	1.81	2.57	2.05	69.3	90.9	−2308.856 86
				Nonlocal (BVWN)			
Cr_2O, C_{2v}	1	1.90		1.74	54.4		−2166.420 40
	3	1.85		1.82	59.1		−2166.428 81
	5	1.86		1.95	63.2		−2166.420 61
Cr_2O_2, D_{2h}	1	1.82	3.05	1.98	65.9	114.1	−2242.006 98
	3	1.83	3.06	1.99	66.1	113.9	−2242.012 94
	5	1.82	2.90	2.20	74.2	105.8	−2242.017 40
	7	1.85	2.95	2.24	74.5	105.5	−2242.042 79
Cr_2O_3, D_{3h}	1	1.83	2.51	2.23	75.0	86.8	−2317.548 82
	3	1.85	2.59	2.17	72.0	89.0	−2317.543 58
	5	1.87	2.68	2.10	68.3	91.6	−2317.572 80

containing the three oxygens. The symmetry of this molecule is C_{3v} (slightly distorted D_{3h}), compatible with that tentatively suggested (C_{3v} or D_{3h}) by Chertihin et al.[5] The introduction of the third oxygen atom lowers the O−Cr−O bond angle and consequently decreasing the O−O distance, as the R_{Cr-O} distance almost maintains the value computed in the diatomic and triatomic molecules. For the CrO_3 cluster, we found the singlet spin state to be the ground state.

3.1.2. Cr_2O, Cr_2O_2, and Cr_2O_3. The Cr_2O cluster has approximately the geometry of an equilateral triangle within the symmetry of the C_{2v} point group (see Table 3). The ground state is a triplet spin state. R_{Cr-O} increases with respect to CrO_2 by about 0.2 Å, indicating the presence of a weaker Cr−O bond. The separation between the two Cr atoms becomes only 0.13 Å larger than the computed value for the Cr_2 dimer. It should be noticed that for Cr_2 the experimental R_{Cr-Cr} distance (1.68 Å, ref 25) is found to be only 0.01 Å higher in our calculation. These results manifest that intermetallic interactions are present in the molecule, as we will show later. Thus, the bond angle for this triatomic reduces to 59.1° as compared with the value 131.1° of the oxygen-excess triatomic. We would like to emphasize that our prediction is in contrast to the estimated value of 138° given by Chertihin et al.[5] Their estimation is based on a tentative assignment of the 804 cm^{-1} band to the antisymmetric mode of the Cr_2O molecule.

For the Cr_2O_2 and Cr_2O_3 clusters, we obtain Cr−O separations similar to the metal-excess triatomic, although in these two clusters the Cr−Cr distance and the Cr−O−Cr angle increase to accommodate the new interactions. As in the triatomic molecule, competition between different spin states is greater than that in the CrO_n series (see Table 3). Septet and quintet spin states have been obtained as the ground states for Cr_2O_2 and Cr_2O_3, respectively. We have also found slight discrepancies with the experimental work of Chertihin et al.[5] concerning their molecular structures. The proposed geometries after infrared frequency assignments could be seen respectively as distortions of our D_{2h} and D_{3h} optimized configurations. For Cr_2O_2, the distortion would probably lead to a nonplanar C_{2v} structure (instead of D_{2h}), whereas for Cr_2O_3 the distortion would be greater since the suggestion is a puckered Cr_2O_2 ring with one terminal O atom.[5] In fact, our vibrational analysis of the Cr_2O_3 cluster shows that there is one imaginary frequency, with a small magnitude (<100 cm^{-1}). The negative value for the second derivative of the cluster energy may be due by the loss of precision in the computations of flat energy curves for this cluster. Besides, the corresponding normal mode does not indicate a movement of the atoms in the direction of the proposed distortion based on experiments. From the above comments, it seems clear that further work on the structural properties of the Cr_2O_3 cluster is warranted.

3.2. Chemical Bonding. The wave functions of the ground states discussed above contain the electronic structure information of these clusters. Our aim here is not to describe in detail all of this information but to point out the most relevant aspects concerned mainly with the chemical bonding. There are some important features that are common for all the clusters and will be used to brief our discussion. For example, we have found that in all the cases the analysis of the chemical bonding can reasonably be performed by considering only the four and six valence electrons of oxygen and chromium, respectively. Thus, the interesting valence molecular orbitals (MOs) are mainly built up with contributions only from the 2p oxygen atomic orbitals ($2p_O$) and 3d chromium atomic orbitals ($3d_{Cr}$). This is illustrated in the density of state (DOS) plots (Figures 2 and 3) where the total DOS in the valence region (up to 5 eV below the energy of the corresponding highest occupied MO (HOMO)) can approximately be generated by contributions from the $3d_{Cr}$ and the $2p_O$ orbitals.

Each of these MOs can be classified into one of the following four types, in order of increasing energy: (i) Nonbonding $2p_O$ MOs (NB−O): they are doubly occupied, and there are as many as oxygen atoms in the cluster. (ii) Bonding $2p_O - 3d_{Cr}$ MOs (B−O−Cr): they are also doubly occupied and are dominated by the oxygen contribution. The polar character of these covalent bonds is due to the greater electronegativity of the O atom with respect to the Cr, as indicated by the difference between the $2p_O$ and $3d_{Cr}$ orbital energies. The number of B−O−Cr MOs is always twice the number of oxygens in the cluster. (iii) Bonding $3d_{Cr} - 3d_{Cr}$ MOs (B−Cr−Cr): they are present only in the Cr_2O_n series and are doubly occupied. (iv) Nonbonding $3d_{Cr}$ MOs (NB−Cr): these MOs are singly occupied and are the ones with highest orbital energies. In the last two cases, there exists a variable contamination in the MOs due to the contribution of $2p_O$ orbitals.

Having these considerations in mind, we can start by writing down the electronic valence configuration of the CrO_n clusters which for CrO is $(NB-O)^2\ (B-O-Cr)^4\ (NB-Cr)^4$, for CrO_2 is $(NB-O)^4\ (B-O-Cr)^8\ (NB-Cr)^2$, and for CrO_3 is $(NB-O)^6\ (B-O-Cr)^{12}$.

Note that in these clusters the number of electrons in the outer nonbonding MOs decreases as the number of O atoms increases. This fact correlates with the increase of the number of electrons in bonding MOs in the same direction, giving CrO_3 a closed-shell structure. Nevertheless, the effective number of electrons per Cr−O bond is four in these clusters. Given the simplicity of our premises, our proposed valence configurations are in good agreement with the calculated Mayer bond orders[26] collected in Table 4. It is also to be noticed that besides the Cr−O bond orders, the Mulliken charge (see also Table 4) associated with the oxygen maintains a value around −0.6 *e* for the three clusters. The deformation density maps in Figure 4 show the corresponding regions that either gain or loss of electronic charge upon bond formation. It is apparent that transfer of electronic density occurs from Cr to O atoms (almost exclusively from $3d_{Cr}$ and $4s_{Cr}$ to $2p_O$) with no accumulation between oxygens.

Globally, we can say that the bonding in these clusters is characterized by almost independent, covalent, and polarized double bonds between Cr and O, with negligible values of O−O bond orders. In this respect, we recall the similar R_{Cr-O} distances and the large O−O separations computed for this series. Further, the strength of the Cr−O bond (around 5 eV) confers to these clusters a high stability, with large HOMO−LUMO gaps (around 1 eV, see Table 4). This is in agreement with the principle of maximum hardness[27] which relates hard molecules with high HOMO−LUMO differences.

The CrO_n series also shows a regular trend in terms of the orbital energies, as illustrated in Figure 5. Passing from CrO to CrO_3 leads to a shift of all the orbitals to lower energies. This is a consequence of the increase in the $2p_O$ character of the outer valence orbitals. Thus, the HOMO moves from −4.5 eV in CrO to −6.3 eV in CrO_2, and to −8.1 eV in CrO_3. These values can be used to estimate the trend of the first ionization potential in these clusters. This effect is clearly illustrated in Figure 2: as the number of O atoms increases, a gradual decreasing of the $3d_{Cr}$ participation in the total DOS accompanied by an increasing of the $2p_O$ participation occurs.

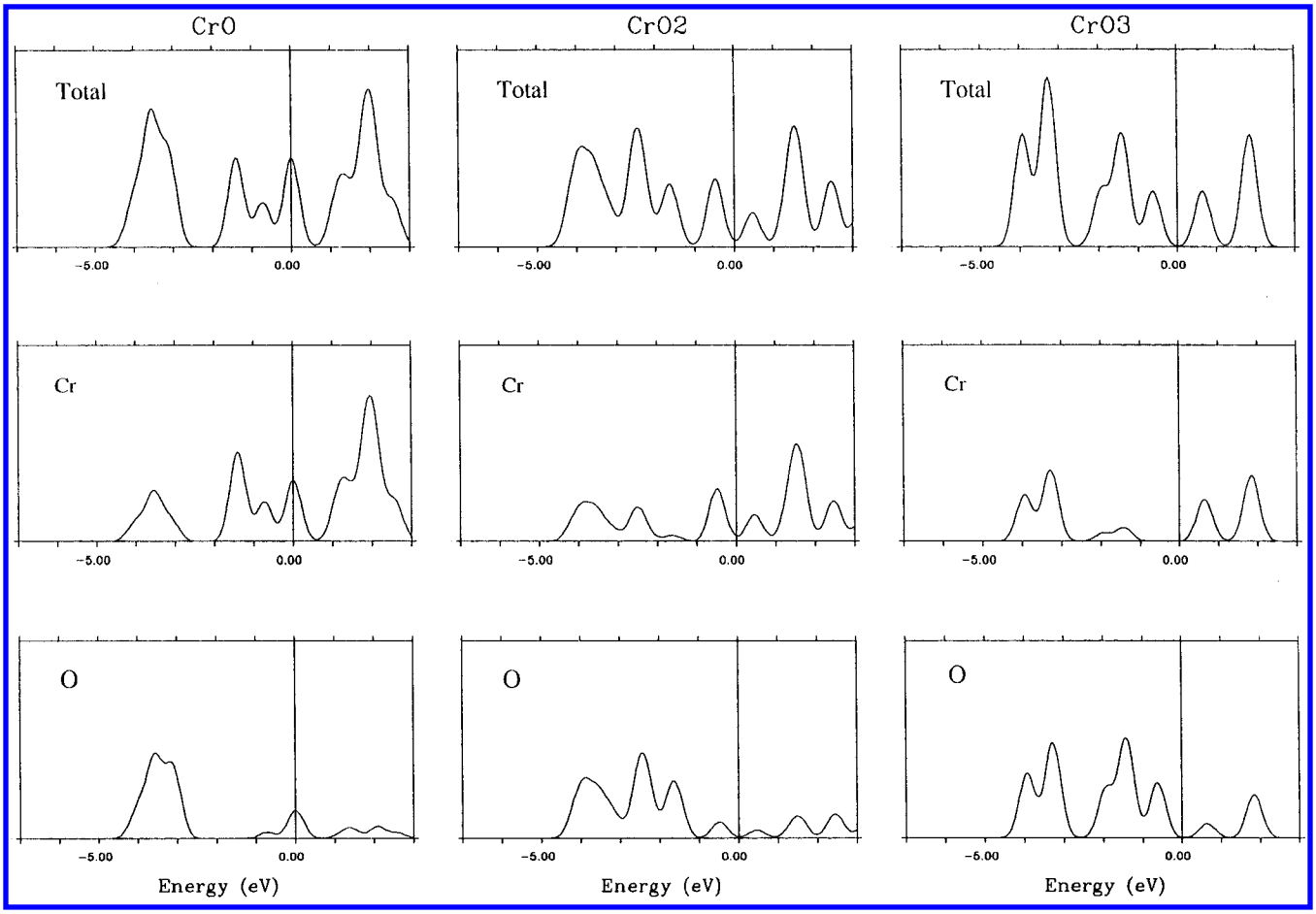

Figure 2. Total and partial ($3d_{Cr}$ and $2p_O$) density of state plots for CrO_n clusters of Figure 1. We have scaled the heights of the plots according to the number of the valence electrons in each cluster.

Notice that for the closed-shell CrO_3 cluster the upper valence level is completely dominated by the $2p_O$ orbitals.

For the Cr_2O_n series, the electronic valence configurations can be written as $(NB-O)^2$ $(B-O-Cr)^4$ $(B-Cr)^8$ $(NB-Cr)^2$ for Cr_2O, $(NB-O)^4$ $(B-O-Cr)^8$ $(B-Cr)^2$ $(NB-Cr)^6$ for Cr_2O_2, and $(NB-O)^6$ $(B-O-Cr)^{12}$ $(B-Cr)^2$ $(NB-Cr)^4$ for Cr_2O_3. The number of Cr−O bonds in Cr_2O, Cr_2O_2, and Cr_2O_3 is respectively 2, 4, and 6, which correlates with the number of electrons in the B−O−Cr MOs: 4, 8, and 12. Thus, single Cr−O bonds are suggested in our simple scheme. According to the number of B−Cr electrons, the Cr−Cr bond is quadruple in Cr_2O but single in the other two cases. A reasonable concordance is again found with the calculated Mayer bond orders collected in Table 4. Furthermore, Mulliken O charge remains approximately the same in this series, with a value of −0.80 *e*, which is less than the double of the one obtained for the CrO_n clusters. This is an indication of the decrease in the Cr−O charge transfer in the Cr_2O_n series. In the deformation density maps (see Figure 6), the increase of electronic density at the oxygen sites is now accompanied by accumulation of the electronic density along the Cr−Cr bond. This new feature is especially clear in the Cr_2O cluster.

Our description of the bonding in this series yields again polar roughly independent covalent Cr−O bonds, but less strong and less polarized than before. Besides, the Cr−Cr bonds appear, although they are weaker than in the dimer Cr_2 where a bond order of six is found. This is consistent with the large Cr−Cr separations found in the clusters of this family. In essence, there is a loss in the stability of these clusters with respect to the CrO_n ones that is also illustrated by smaller HOMO−LUMO gaps (see Table 4).

With regards to the valence orbital energies and the nature of the outer MOs, a dominance of the $3d_{Cr}$ orbitals is found. The participation of the $2p_O$ orbitals becomes only important in the deeper valence region as illustrated by the total and partial DOS (see Figure 3). In contrast with the CrO_n series, there is not appreciable shift of the MO levels as the number of O atoms increases, and a value by about −4 eV is obtained for the HOMO orbitals (see Figure 5). Therefore, a lower and constant value for the first ionization potential of these bimetallic oxide clusters is proposed.

3.3. Stability. In this last subsection, we address the question of the stability of the isomers computed in this study. First, we concentrate on the intrinsic stability of the clusters by reporting the analysis of the cluster vibrations. Second, we focus on the relative stability of the clusters by evaluating the binding energies and the energetics of different fragmentation paths.

3.3.1. Cluster Harmonic Vibrations. We have computed the harmonic frequencies and normal modes of all the isomers collected in Tables 2 and 3 for the ground-state equilibrium geometries found in the NLSDA calculations. In the cases of linear isomers of CrO_2, CrO_3, and Cr_2O, we have found several imaginary frequencies with large magnitude for each of them that indicate that these configurations are not true minima on their respective potential energy surfaces. For the linear Cr_2O_2 isomer, we have not even obtained convergence in the self-consistent calculations. The results obtained for the rest of the clusters (Figure 1) are collected in Table 5. It is to be noted that DMol requires the C_1 symmetry to compute the harmonic

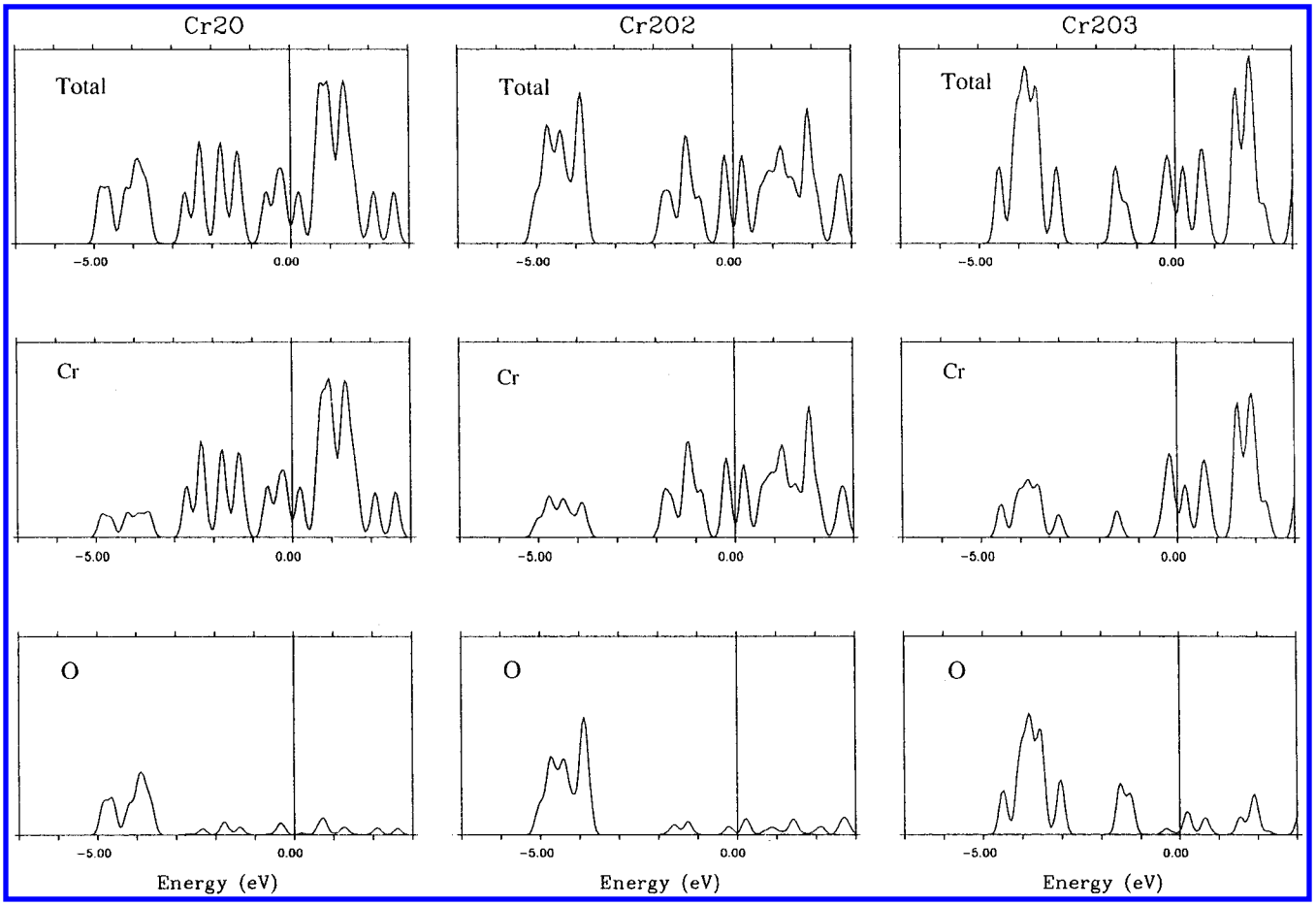

Figure 3. Total and partial ($3d_{Cr}$ and $2p_O$) density of state plots for Cr_2O_n clusters of Figure 1. We have scaled the heights of the plots according to the number of the valence electrons in each cluster.

TABLE 4: Mulliken Charges, Mayer Bond Orders, and HOMO−LUMO Gaps of Cr_mO_n Clusters

cluster	Mulliken charge		bond order			HOMO−LUMO gap (eV)
	Cr	O	Cr−O	O−O	Cr−Cr	
CrO, $C_{\infty v}$	0.64	−0.64	1.81			1.12
CrO_2, C_{2v}	1.25	−0.63	1.82	0.33		0.94
CrO_3, C_{3v}	1.60	−0.54	1.76	0.22		1.26
Cr_2O, C_{2v}	0.40	−0.80	0.98		3.93	0.33
Cr_2O_2, D_{2h}	0.81	−0.81	0.95		1.35	0.43
Cr_2O_3, D_{3h}	1.13	−0.75	0.93		1.10	0.45

frequencies. We have seen that the expected degenerate E modes in CrO_3 and Cr_2 O_3 clusters show a split of only 2−3 cm^{-1} for the higher frequencies, but as large as 20−30 cm^{-1} for the E'' frequency in Cr_2O_3. The average values for these degenerate modes are given in Table 5. Changing the computational parameters that control the evaluation of the second derivatives does not improve the accuracy of the calculations. In this respect, the one missing normal mode for Cr_2O_3 (A_2'') was found to have a magnitude for the imaginary frequency below 100 cm^{-1}.

A simple analysis of the cluster vibrations can be performed considering the metal−oxygen bonds as independent harmonic oscillators controlled by the mass and the force constant.[2] In our case, this strategy is very appropriate given the character of the chemical bonding shown by these clusters. In the CrO_n family, the frequency of the corresponding breathing modes remains around 900 cm^{-1}, which illustrates again the independence of the Cr−O bonds. In the Cr_2O_n series, there is a greater variation of this frequency which can be associated to the changes in the coordination number of chromium and oxygen atoms and in the different strength that the Cr−Cr bond manifests in these clusters. Going from the CrO_n to the Cr_2O_n series implies an increase in the effective mass of the clusters and a loss of the Cr−O bond strength. Accordingly, the frequencies show an overall shift to lower values. This is specially clear for the total symmetric normal modes but needs a more detailed discussion for other modes due to the involvement of the Cr−Cr bond. As a simple example, we consider the CrO_2 and Cr_2O triatomics. The two stretching symmetric and antisymmetric normal modes are higher in frequency in CrO_2, as expected from our previous discussion. On the other hand, the A_1 bending mode is lower when the two like atoms do not show an appreciable interaction (268 cm^{-1} for CrO_2) than when the Cr−Cr bond is present (355 cm^{-1} for Cr_2O). It should be noted that the experimental and our computed frequency for Cr_2 are 470 cm^{-1} (ref 9) and 365 cm^{-1}, respectively.

Comparison with experimental data is possible for all of the normal modes of CrO_2. Very recently, Wenthold et al.[4] reported the values of 895 ± 20 and 220 ± 20 cm^{-1} for the frequencies of the two symmetric modes of this molecule. Chertihin et al.[5] assigned the frequencies of 965.4 and 914.4 cm^{-1} to the antisymmetric and symmetric stretching modes of CrO_2, respectively. Our calculated numbers (975 cm^{-1} (B_1), 900 cm^{-1} (A_1), and 268 cm^{-1} (A_1)) are in good agreement with both sets of data. Especially important is the concordance of the computed frequency at 900 cm^{-1}, since previous infrared experiments[7] reported a value of 960.2 cm^{-1} for this symmetric stretching mode. For the degenerate stretching normal mode of CrO_3, a frequency of 968.4 cm^{-1} is assigned based on infrared

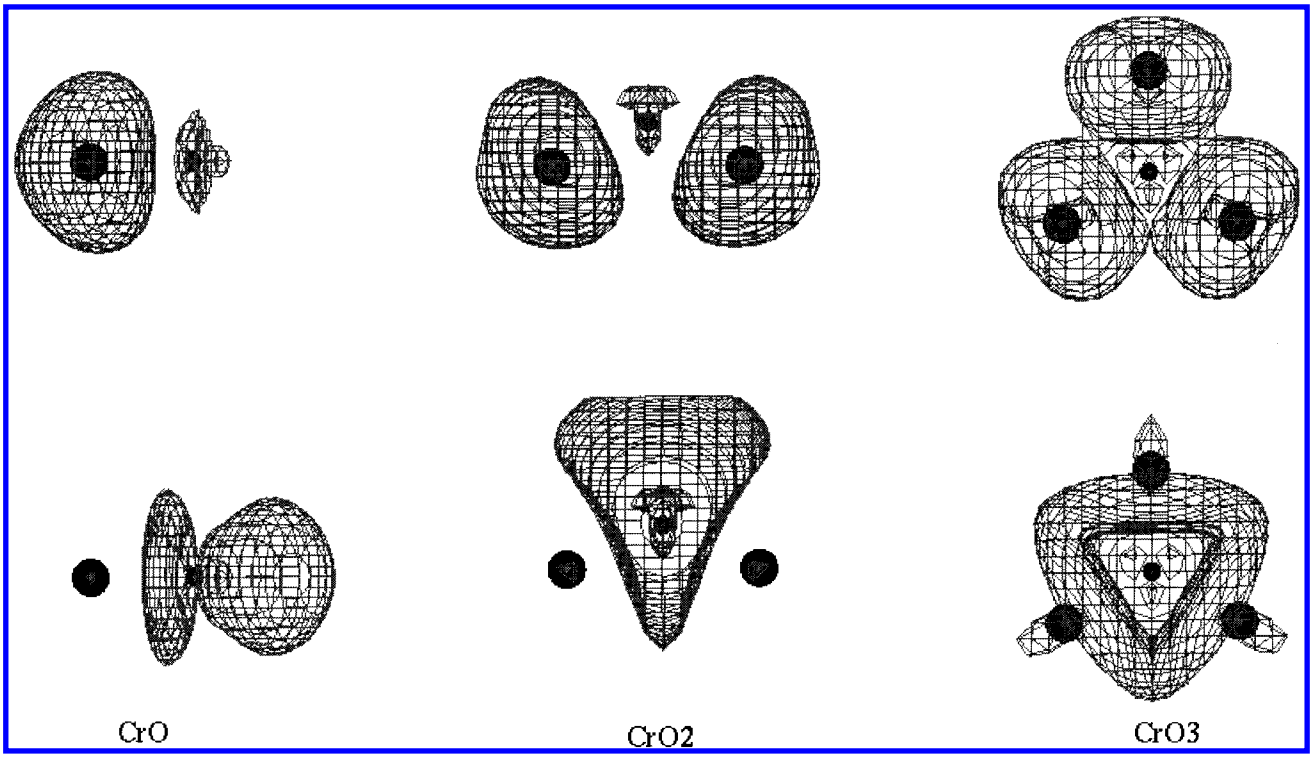

Figure 4. Deformation electronic density maps for CrO_n clusters of Figure 1. Positive (above) and negative (below) regions are plotted. Contour level used is ± 0.001 e/bohr^3.

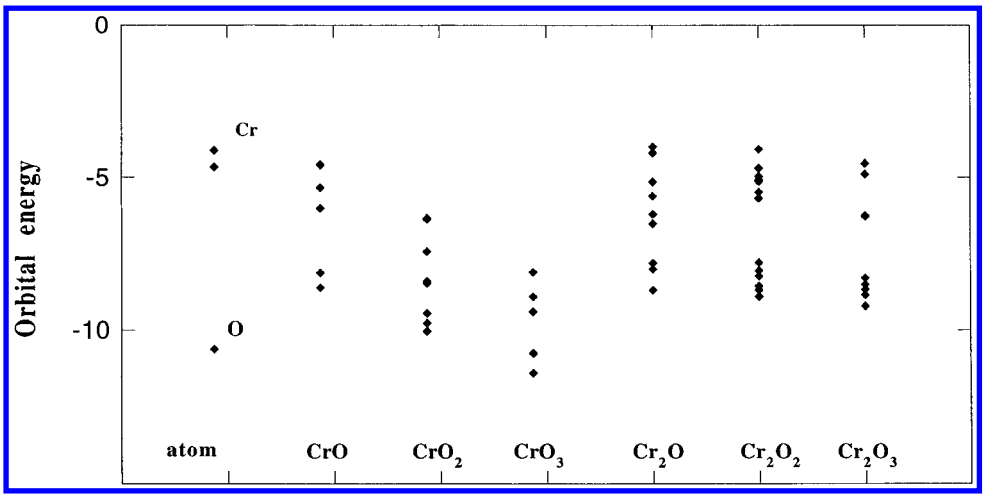

Figure 5. Orbital energies (eV) for outer valence orbitals of the CrO_n and Cr_2O_n clusters of Figure 1.

experiments.[5] Our calculations confirm the assignment, although the computed value is higher by about 25 cm^{-1}. The computed frequency for the stretching A_1 mode (900 cm^{-1}) of this cluster seems also to be very reasonable given the expected similarities in the vibrations of the CrO_2 and CrO_3 clusters.

For the Cr_2O_n clusters, the agreement with the infrared data is not expected since the structures proposed are different. However, it may be still worthwhile to compare our numbers with the experimental ones, at least for Cr_2O and Cr_2O_2. Thus, the weak, broad 804 cm^{-1} band detected by Chertihin et al.[5] and tentatively assigned to the antisymmetric B_1 mode of Cr_2O contrasts with our low predicted value for the frequency of this mode (529 cm^{-1}). In fact, our calculations give a higher frequency for the stretching symmetric mode (774 cm^{-1}), which is also predicted to be more intense. In recent calculations of Cu_2O vibrations,[10] it has been found that the stretching A_1 mode has a higher frequency that the B_1, as in our case. We think that the experiment−theory disagreement may be explained as due to the different prediction for the bond angle in this cluster. Chertihin et al.[5] tentatively assign a 628.2 cm^{-1} band to Cr_2O_2, close to our intense B_{2u} vibration at 678 cm^{-1}. Note that the calculations are in a D_{2h} structure, whereas the proposed configuration in the infrared experiments is also cyclic but nonplanar. We also want to remark that the lowest computed frequency for this cluster (213 cm^{-1}) corresponds to the normal mode vibrating out of the molecular plane. In the case of Cr_2O_3, we have found that the breathing mode is the one with the highest frequency, which is also the result obtained after the calculations of Wang et al.[10] in the corresponding copper cluster.

3.3.2. Binding Energies and Fragmentation Energetics. For $(MgO)_n$ and $(BN)_n$ aggregates,[28−30] we have shown that the analysis of the variation of the atomization and binding energies of clusters with the cluster size provides some insight on the energetics of the nucleation process and on their relative stability, respectively. The atomization energy is defined as the total energy with respect to the atomic constituents, whereas

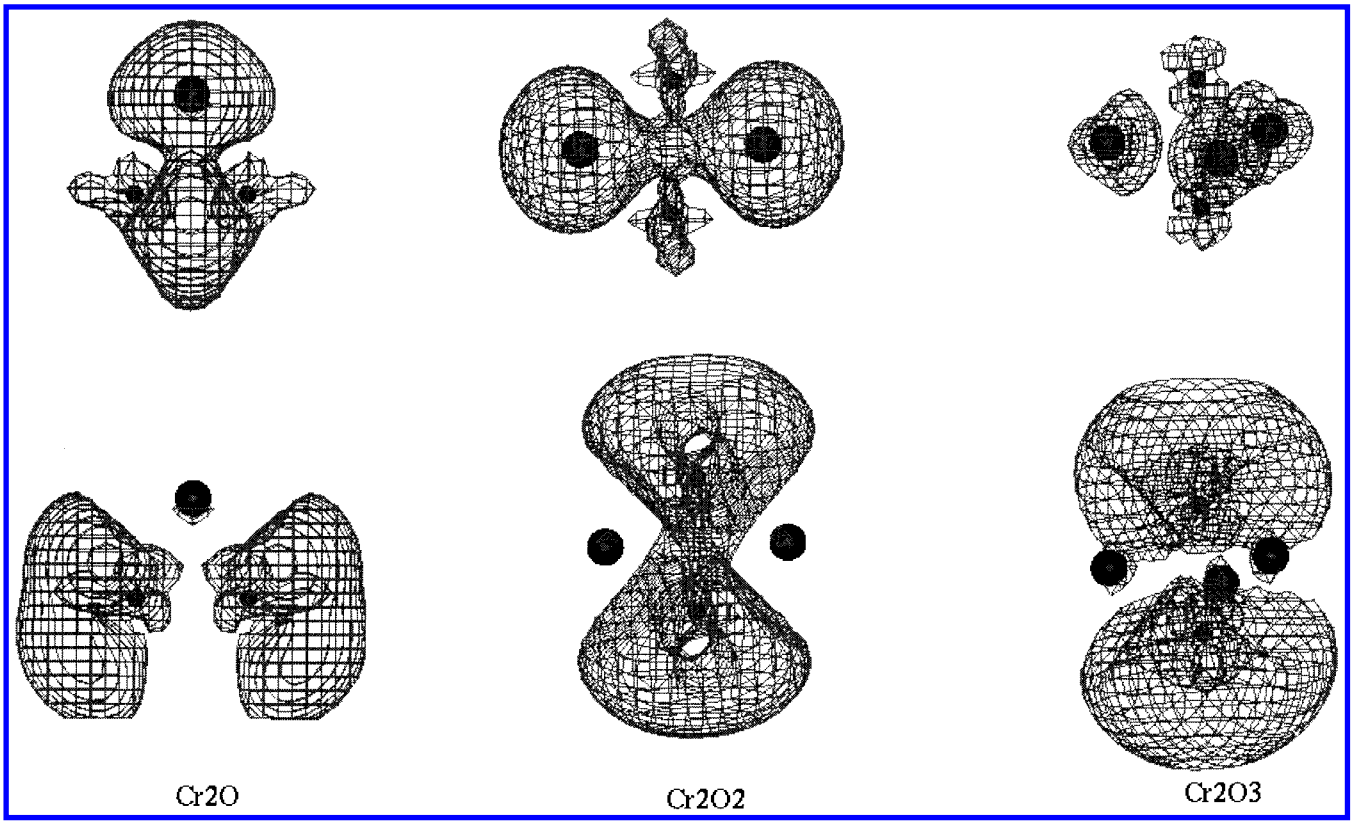

Figure 6. Deformation electronic density maps for Cr_2O_n clusters of Figure 1. Positive (above) and negative (below) regions are plotted. Contour level used is ±0.001 e/bohr^3, except for Cr_2O_3 which is ±0.015 e/bohr^3.

TABLE 5: Calculated Normal Modes of Cr_mO_n Clusters ($m = 1-2$, $n = 1-3$)

cluster	mode	freq (cm^{-1})	rel IR intensity
CrO, $C_{\infty v}$	A_1	884	1
CrO_2, C_{2v}	A_1	268	0.08
	A_1	900	0.05
	B_1	975	1
CrO_3, C_{3v}	A_1	132	0.41
	E	345	0
	A_1	900	0.03
	E	992	1
Cr_2O, C_{2v}	A_1	355	0.07
	B_1	529	0.3
	A_1	774	1
Cr_2O_2, D_{2h}	B_{1u}	213	0.1
	A_{1g}	243	0.0
	B_{1g}	422	0.0
	B_{3u}	486	0.9
	A_{1g}	675	0.0
	B_{2u}	678	1.0
Cr_2O_3, D_{3h}	E″	115	0.0
	E′	296	0.2
	A_1'	491	0.0
	E′	652	1.0
	A_1'	721	0.0

the binding energy refers to the total energy per diatomic molecule. Clearly, for the clusters studied here this binding energy has to be redefined for each of the two CrO_n and Cr_2O_n series in terms of the number of oxygen atoms.

Concerning the atomization energies, we observe that the growing of the clusters by adding either one Cr or one O atom is always a favorable process. Thus, starting with the two separate atoms, the NLSDA atomization energy increases (in absolute value of electronvolts) following this sequence: CrO (5.10), Cr_2O (5.52), Cr_2O_2 (12.67), and Cr_2O_3 (17.54). It is clear that the gain in energy is greater when one oxygen atom is attached to the cluster. In this way, it should be noted that the Cr_2O_3 cluster can be obtained through another succession: CrO (5.10), CrO_2 (11.27), CrO_3 (16.52), and Cr_2O_3 (17.54), which is more likely to be preferred. This result may be associated with the fact that only experimental data are available for the atomization energies of the CrO_n family. The tabulated numbers[31] are 4.71, 9.98, and 14.8 ± 0.4 eV for CrO, CrO_2, and CrO_3, respectively, and show an overestimation by the calculations that on the other hand follow an appropriate correct trend.

When the binding energy is considered, we obtain the values of 5.10, 5.64, and 5.51 eV for CrO, CrO_2, and CrO_3, respectively. Accordingly, the CrO_2 triatomic is found to have an enhanced stability in this series that should be confirmed through the fragmentation energetic analysis. Notice that the tabulated bond orders in Table 4 are in concordance with the above result for CrO_2, as this is the cluster with the highest bond orders. Further, the peak for the triatomic is also present in the experimental values. For the Cr_2O_n family, the corresponding numbers are 5.52, 6.34, and 5.85 eV. Again, the cluster with two oxygen atoms coordinated to the chromium is the most stable one.

Evaluation of the fragmentation energetics of these clusters with regard to all possible pathways support the above results. The picture is consistent in both local and nonlocal approximations. The fragmentation path energies computed in the nonlocal approximation are

$$\begin{aligned} &CrO \rightarrow Cr + O\ (5.1\ eV),\\ &CrO + O \rightarrow Cr + O_2\ (-0.77\ eV) \end{aligned} \qquad (A)$$

$$\begin{aligned} &CrO_2 \rightarrow CrO + O\ (6.16\ eV),\\ &CrO_2 \rightarrow Cr + O_2\ (5.39\ eV) \end{aligned} \qquad (B)$$

$$CrO_3 \rightarrow CrO_2 + O\ (5.26\ eV),$$
$$CrO_3 \rightarrow CrO + O_2\ (5.55\ eV) \qquad (C)$$

$$Cr_2O \rightarrow Cr_2 + O\ (5.00\ eV),$$
$$Cr_2O \rightarrow CrO + Cr\ (0.41\ eV) \qquad (D)$$

$$Cr_2O_2 \rightarrow CrO + CrO\ (2.46\ eV),$$
$$Cr_2O_2 \rightarrow Cr_2 + O_2\ (6.28\ eV)$$
$$Cr_2O_2 \rightarrow Cr_2O + O\ (7.16\ eV),$$
$$Cr_2O_2 \rightarrow CrO_2 + Cr\ (1.40\ eV) \qquad (E)$$

$$Cr_2O_3 \rightarrow Cr_2O_2 + O\ (4.87\ eV),$$
$$Cr_2O_3 \rightarrow Cr_2O + O_2\ (6.15\ eV)$$
$$Cr_2O_3 \rightarrow CrO_2 + CrO\ (1.17\ eV),$$
$$Cr_2O_3 \rightarrow 2CrO + O\ (7.33\ eV)$$
$$Cr_2O_3 \rightarrow CrO_3 + Cr\ (1.01\ eV) \qquad (F)$$

From the above reactions, we would like to emphasize the following: (i) Looking at the most favorable paths to break the clusters, CrO_2 and Cr_2O_2 have the highest values (5.39 and 1.40 eV, respectively) for each series. This is consistent with the binding energy analysis. (ii) Comparison with the available experimental information shows both quantitative and qualitative agreement with our results. Thus, the reported exothermic character of the CrO + O reaction (−0.74 eV)[25] is obtained in our computations. In the same way, the expected high endothermicity for the reactions[31] under the (C) label are predicted here to have values of about 5.4 ± 0.1 eV. There is also concordance between the experimental value (−113 ± 11 kcal/mol, ref 31) and the theoretical one (−124 kcal/mol) for the Cr + O_2 reaction. (iii) The dissociation of Cr_2O appears to have the lowest fragmentation energy followed by the dissociation of Cr_2O_3 and Cr_2O_2. Overall, the results predict a preference for evaporation of Cr over loss of O, which is in the direction of the reported lack of metal-rich clusters in the experimental mass spectra.[3] We should indicate that our NLSDA calculations underestimate the Cr_2 binding energy by about 1 eV. However, this result does not modify the above conclusion since the same preference is found when LSDA computations (that agrees with the experimental binding energy of Cr_2) are used to evaluate the fragmentation energies. (iv) For CrO_3 and Cr_2O_3, the dissociation of clusters into a CrO_2 subunit and a corresponding fragment appears to be favorable, suggesting it as a prime candidate for the basic building block of the larger Cr_mO_n clusters.

4. Conclusions

We have shown that the use of appropriate computational parameters (e.g., basis sets, functionals, active valence space) under the DFT framework provides a satisfactory global description of structural, electronic, and energetic properties of small size chromium oxide clusters. Our results show significant differences between the chemistry of the CrO_n and Cr_2O_n series as illustrated in the trends of the cluster bonding, the cluster vibrations, and the fragmentation energetics. The calculated geometries and vibrational frequencies for the CrO_n family support the available experimental data, while for the Cr_2O_n family a more detailed experimental and theoretical investigation is suggested to confirm or refine our predictions.

We have proposed a simple description of the MOs in terms of contributions only from $2p_O$ and/or $3d_{Cr}$ atomic orbitals that accounts for many different aspects concerning the chemical bonding of the clusters considered here. The Cr−O bonds appear to be stronger in the CrO_n series than in the Cr_2O_n one, where the Cr−Cr bond is found to be a differential feature. However, in all the cases the Cr−O bond is seen to behave independently due to their polar covalent character. This fact allows us to carry out a reasonable analysis of the cluster vibrations using the mass and the bond strength as the only key parameters. This analysis explains the similar frequencies found for the breathing modes of the CrO_n clusters and the lower vibrational frequencies shown by the bimetallic oxide clusters. From the electronic and vibrational study, we conclude that the chemical stability is greater for the CrO_n family.

Our detailed study of atomization, binding, and fragmentation energies has revealed that enriching the clusters with O is preferred over Cr, the loss of Cr atoms is the most appropriate channel to break the Cr_2O_n clusters, and the CrO_2 unit may be considered as a primary building block for the nucleation of chromium oxide clusters. All this results are consistent with the detected preference of oxygen-rich chromium clusters in a variety of experimental investigations.[3,5,7]

Acknowledgment. The authors express their gratitude to Dr. M. A. Van Daelen for his help with the DMol program. J.M.R. wants to express his gratitude to the Ministerio de Educacion y Cultura (DGES) of Spain and NATO collaborative grant No. CRG921348 for financial support during his stay at Michigan Technological University. S.V. acknowledges financial assistance in the form of a fellowship from MSI and Michigan Technological University. Spanish DGICYT, Project PB96-0559, is also acknowledged.

References and Notes

(1) Brandle, H.; Weller, D.; Parkin, S. S. P.; Scott, J. C.; Fumagalli, P.; Reim, W.; Gambino, R. J.; Ruf, R.; Guntherodt, G. *Phys. Rev. B* **1992**, *46*, 221.

(2) Torrent, M.; Gili, P.; Durand, M.; Solà, M. *J. Chem. Phys.* **1996**, *104*, 9499.

(3) Niemann, G. C.; Parks, E.; Richtsmeier, S.; Liu, K.; Pobo, L.; Riley, S. *High Temp. Sci.* **1986**, *22*, 115.

(4) Wenthold, P. G.; Jonas, K. L.; Lineberg, W. C. *J. Chem. Phys.* **1997**, *106*, 9961.

(5) Chertihin, G. V.; Bare, W. D.; Andrews, L. *J. Chem. Phys.* **1997**, *107*, 2798.

(6) Grimley, R. T.; Burns, R. P.; Inghram, M. G. *J. Chem. Phys.* **1961**, *34*, 664.

(7) Almond, M. J.; Hahne, M. *J. Chem. Soc., Dalton Trans.* **1988**, 2255.

(8) Ziemann, P. J.; Castleman, A. W. J. *Phys. Rev. B* **1992**, *46*, 13480.

(9) Salahub, D. R. In *Advances in Chemical Physics*; Lawley, K. P., Ed.; John Wiley and Sons: Chichester, 1987; Vol. LXIX, p 447.

(10) Wang, L. S.; Wu, H.; Desai, S. R. *Phys. Rev. B* **1996**, *53*, 8028.

(11) Bauschlicher, C.; Nelin, C.; Bagus, P. *J. Chem. Phys.* **1985**, *82*, 3265.

(12) Bauschlicher, C.; Maitre, P. *Theor. Chim. Acta* **1995**, *90*, 189.

(13) Broclawik, E. *Catal. Today* **1995**, *23*, 379.

(14) *DMol user guide*, version 2.3.6, MSI, 1995.

(15) Delley, B.; Freeman, A. J.; Ellis, D. E. *Phys. Rev. Lett.* **1983**, *50*, 488.

(16) Delley, B. *J. Chem. Phys.* **1990**, *92*, 508.

(17) Li, Y.; Van Daelen, M.; King-Smith, D.; Wrinn, M.; Wimmer, E.; Newsam, J.; Klitsner, T.; Sears, M.; Carlson, G.; Nelson, J.; Allan, D.; Teter, M. Density functional methods and applications to materials problems. In *Electronic Packaging Materials Science VII Symposium*; Borgesen, P., Jensen, K., Pollak, R., Eds.; Materials Research Society: Pittsburgh, PA, 1994; pp 233−43.

(18) Veliah, S.; Pandey, R.; Li, Y.; Newsam, J.; Vessal, B. *Chem. Phys. Lett.* **1995**, *235*, 53.

(19) Moruzzi, V.; Janak, J.; Williams, A. *Calculated Electronic Properties of Metals*, Pergamon: Oxford, UK, 1978.

(20) Vosko, S. H.; Wilk, L.; Nusair, M. *Can. J. Phys.* **1980**, *58*, 1200.

(21) Becke, A. D. *Phys. Rev. A* **1988**, *38*, 3098.

(22) Perdew, J. P.; Yue, W. *Phys. Rev. B* **1986**, *33*, 8800.

(23) Jasien, P.; Stevens, W. J. *Chem. Phys. Lett.* **1988**, *147*, 72.
(24) Steimle, T. C.; Nachman, D. F.; Shirley, J. E.; Bauschlicher, C.; Langhoff, S. R. *J. Chem. Phys.* **1989**, *91*, 2049.
(25) Huber, K P.; Herzberg, G. *Constants of Diatomic Molecules*, Van Nostrand: New York, 1979.
(26) Mayer, I. *Chem. Phys. Lett.* **1983**, *97*, 270.
(27) Pearson, R. G. *Acc. Chem. Res.* **1993**, *26*, 250.
(28) Recio, J. M.; Pandey, R. *Phys. Rev. A* **1993**, *47*, 2075.
(29) Recio, J. M.; Pandey, R.; Ayuela, A.; Kunz, A. B. *J. Chem. Phys.* **1993**, *98*, 4783.
(30) Sutjianto, A.; Pandey, R.; Recio, J. M. *Int. J. Quantum Chem.* **1994**, *52*, 199.
(31) *J. Phys. Ref. Data* **1985**, *14*, (Supp. 1), 938. *JANAF Thermochemical Tables*, 3rd ed., Dow Chemical Company: Midland, 1985.